Liquid Crystals
Publication details, including instructions for authors and subscription information:
http://www.informaworld.com/smpp/title~content=t713926090

Theoretical study of layer alignment in shear flow of smectic A liquid crystals

T. Carlsson[a]; F. M. Leslie[b]
[a] Physics Department, Chalmers University of Technology, Göteborg, Sweden [b] Department of Mathematics, University of Strathclyde, Glasgow, Scotland

To cite this Article Carlsson, T. and Leslie, F. M.(1996) 'Theoretical study of layer alignment in shear flow of smectic A liquid crystals', Liquid Crystals, 20: 6, 697 — 704
To link to this Article: DOI: 10.1080/02678299608033162
URL: http://dx.doi.org/10.1080/02678299608033162

LIQUID CRYSTALS, 1996, VOL. 20, NO. 6, 697–704

Theoretical study of layer alignment in shear flow of smectic A liquid crystals

by T. CARLSSON*

Physics Department, Chalmers University of Technology, S-412 96 Göteborg, Sweden

and F. M. LESLIE

Department of Mathematics, University of Strathclyde, Livingstone Tower, 26 Richmond Street, Glasgow G1 1XH, Scotland

(*Received 18 September 1995; accepted 18 December 1995*)

This paper presents a theoretical study of the behaviour of smectic A liquid crystals subject to shear flow. The liquid crystal is assumed to consist of uniform, planar smectic layers, on which no external moments and no external boundary conditions have been imposed. It is shown that of the five viscosity coefficients needed for a full description of dynamical behaviour of the S_A phase, only two, λ_1 and λ_4, enter the expression of the shearing torque. A stability analysis establishes the possible flow alignment configurations of the smectic layers, and the geometrical arrangements of the flow aligned smectic layers are depicted, parametrized by the crucial parameter λ_1/λ_4. Finally, the effective viscosities of the system are derived for some fundamental orientations of the smectic layers with respect to the shear plane, and these allow the derivation of a few inequalities that the viscous coefficients should satisfy.

1. Introduction

The director dynamics of the ferroelectric smectic C* (S_C^*) phase have been studied intensively during the past decade. Only recently, however, have the hydrodynamic equations of the S_C^* phase become available in the literature through the work by Leslie *et al.* [1]. Based on this theory, Carlsson *et al.* have investigated the flow properties of the S_C^* phase, assuming that boundary conditions, keeping the smectic layers fixed in space and time, are imposed on the sample [2–4]. In reality, under some circumstances, such boundary conditions might not exist and the layers will start rotating under the influence of a macroscopic flow. The general analysis of this situation turns out to be rather complicated due to the coupling between the rotation of the smectic layer normal and the rotation of the director along the smectic cone. For this reason, in this work we study the rotation of the smectic layers of a smectic A (S_A) liquid crystal subject to shear flow, in order to obtain some knowledge of how the smectic layers may behave in shear flow. We assume throughout the work that the liquid crystal consists of uniform, planar smectic layers, on which no external moments and no external boundary conditions have been imposed.

The outline of the paper is as follows. § 2 gives the basic dynamic equations, needed for the present analysis, including a description of the viscous torque. This section also includes a description of how one of the basic equations can be interpreted as a balance of torque equation. § 3 introduces the coordinates used to describe the system, and also derives the governing equations for the present problem. We show that only two viscous coefficients, denoted λ_1 and λ_4, enter the equations. It is also shown, using thermodynamical reasoning, that the coefficient λ_4 must be positive. In § 4 we demonstrate that for some orientations of the smectic layers, the viscous torque vanishes. These orientations define the possible candidates for what one might call the layer flow alignment angles. In § 5 we discuss the stability of these flow alignment angles, showing that their stability is determined by the ratio λ_1/λ_4. Comparing our results with the behaviour of disc-like nematics in shear flow, we propose in § 4 what we believe is a reasonable assumption for the value of the ratio λ_1/λ_4. Finally, § 7 gives a derivation of the effective viscosities of the system for some geometries of the flow, using the results to derive some additional inequalities for the viscous coefficients.

2. Basic equations: the smectic A stress tensor

In this work we study the dynamics of a S_A liquid crystal, describing the layer normal by a unit vector **a**.

*Author for correspondence.

Assuming that the system is free from dislocations and of constant layer thickness, the layer normal **a** must fulfill the constraint [5]

$$\nabla \times \mathbf{a} = 0. \tag{1}$$

When studying the transport of matter in the system, the liquid crystal is considered to be incompressible, and the velocity field **v** is subject to the constraint

$$\nabla \cdot \mathbf{v} = 0. \tag{2}$$

Apart from this constraint, we allow for any type of flow in the analysis, i.e. we also consider the situation where matter is transported not only within the smectic layers, but also between them.

The continuum theory for the S_A phase can be written down as a special case of that recently proposed by Leslie *et al.* [1, 2] for the S_C phase, simply putting the c-director equal to zero. Given the assumptions of constant layer thickness and imcompressibility, the continuum theory essentially rests on two balance laws for linear and angular momentum, namely

$$\rho \dot{v}_i = F_i + t_{ij,j}, \tag{3}$$

$$\Gamma_i + \varepsilon_{ijk} t_{kj} + l_{ij,j} = 0, \tag{4}$$

where **F** and **Γ** denote external body force and moment per unit volume, and t_{ij} and l_{ij} the stress and couple stress tensors, respectively. Given the constraints the latter can be expressed as

$$t_{ij} = -p\delta_{ij} + \beta_p \varepsilon_{pjk} a_{k,i} - \frac{\partial w}{\partial a_{k,j}} a_{k,i} + \tilde{t}_{ij}, \tag{5}$$

$$l_{ij} = \beta_p a_p \delta_{ij} - \beta_i a_j + \varepsilon_{ipq} a_p \frac{\partial w}{\partial a_{q,j}} + \tilde{l}_{ij}, \tag{6}$$

the pressure p arising from the assumed incompressibility and the vector $\boldsymbol{\beta}$ stemming from the constraints imposed on the smectic layers. Furthermore, $\tilde{t}_{ij}$ and $\tilde{l}_{ij}$ denote dynamic contributions, $\tilde{l}_{ij}$ being proven to be zero [1], while w is the elastic energy of the system given by [5]

$$w = \tfrac{1}{2} K (\nabla \cdot \mathbf{a})^2. \tag{7}$$

In this work we consider a S_A liquid crystal, consisting of uniform, planar smectic layers, on which no external moments and no external boundary conditions have been imposed. Thus the elastic energy w equals zero throughout the sample. The vector $\boldsymbol{\beta}$ which is related to the external torque imposed on the system [2] will also vanish in this case. Thus equations (3)–(6) reduce to

$$\rho \dot{v}_i = F_i + \tilde{t}_{ij,j}, \tag{8}$$

$$\varepsilon_{ijk} \tilde{t}_{kj} = 0. \tag{9}$$

Studying a simple shear flow, equation (8) can be used to calculate the external force, acting on the moving plate, necessary to maintain the flow, while equation (9), which can be interpreted as a balance of torque equation, is the equation governing the behaviour of the smectic layer normal. This is the main equation studied in this work.

Before writing down the S_A stress tensor we introduce the rate of strain and vorticity tensors

$$D_{ij} = \tfrac{1}{2}(v_{i,j} + v_{j,i}), \tag{10}$$

$$W_{ij} = \tfrac{1}{2}(v_{i,j} - v_{j,i}), \tag{11}$$

and the vector **A** related to the material time derivative of the unit vector **a**

$$A_i = \dot{a}_i - W_{ik} a_k. \tag{12}$$

Also we find it convenient to employ the notation

$$D_i^{\mathrm{a}} = D_{ij} a_j. \tag{13}$$

With these definitions the dynamic part of the S_A stress tensor can be written [1, 2]

$$\tilde{t}_{ij} = \tilde{t}_{ij}^{\mathrm{s}} + \tilde{t}_{ij}^{\mathrm{a}}, \tag{14}$$

where

$$\tilde{t}_{ij}^{\mathrm{s}} = \mu_0 D_{ij} + \mu_1 a_p D_p^{\mathrm{a}} a_i a_j + \mu_2 (D_i^{\mathrm{a}} a_j + D_j^{\mathrm{a}} a_i) + \lambda_1 (A_i a_j + A_j a_i) \tag{15}$$

is the symmetric part of the stress tensor and

$$\tilde{t}_{ij}^{\mathrm{a}} = \lambda_1 (D_j^{\mathrm{a}} a_i - D_i^{\mathrm{a}} a_j) + \lambda_4 (A_j a_i - A_i a_j) \tag{16}$$

is the antisymmetric part. We also remind the reader that the usual summation convention is adopted throughout this work.

With the interpretation of equation (9) as a balance of torque equation, we introduce the viscous torque Γ^{v} according to

$$\Gamma_i^{\mathrm{v}} = \Gamma_i^{\mathrm{s}} + \Gamma_i^{\mathrm{r}} = \varepsilon_{ijk} \tilde{t}_{kj}^{\mathrm{a}}. \tag{17}$$

In equation (17) the viscous torque has been divided into two parts: the shearing torque Γ^{s} which is the torque acting on the layer normal due to velocity gradients, and the rotational torque Γ^{r} which is the torque appearing whenever the layer normal is rotating. From the form of $\tilde{t}_{ij}^{\mathrm{a}}$, equation (16), we notice that only two viscosities enter the problem, λ_1 and λ_4. We show later (cf. § 3.3) that stability reasons demand the coefficient λ_4 to be positive,

$$\lambda_4 > 0. \tag{18}$$

3. The shear flow geometry: definition of coordinates and derivation of the governing equations

3.1. *Presentation of the problem and definition of the coordinates*

In this work we study the shear flow of a S_A liquid crystal, assumed to be confined between two parallel glass plates, distance d apart. The coordinates needed to define the problem are introduced in figure 1. The glass plates are taken to be parallel to the xy-plane, one of them being at rest while the other one is moving in the y-direction with the velocity v_0, implying the velocity field to be of the form

$$v_x = 0, \quad v_y = v(z), \quad v_z = 0 \tag{19}$$

The smectic planes are assumed to be uniform and planar, the layer normal being defined by a unit vector $\mathbf{a}$. We thus expect a uniform shear rate $dv/dz \equiv v' = v_0/d$ to be present everywhere in the sample. Furthermore, we do not impose any boundary conditions on the smectic layers, leaving the layer normal free to orient itself in any arbitrary direction.

The orientation of $\mathbf{a}$ can be described by using a spherical polar coordinate system (r, ψ, α) as depicted in figure 1. The angle ψ is an angle between $\mathbf{a}$ and the y-axis, while α is the angle which the projection of the layer normal onto the xz-plane makes with the x-axis, counting α positive for rotations around the positive y-axis. With these definitions, $\mathbf{a}$ can be written as

$$\mathbf{a} = \hat{x}\sin\psi\cos\alpha + \hat{y}\cos\psi - \hat{z}\sin\psi\sin\alpha \tag{20}$$

Associated with the coordinate system introduced above there belongs a set of bases vectors, $\hat{\mathbf{r}}$, $\hat{\mathbf{\Psi}}$ and $\hat{\boldsymbol{\alpha}}$,

$$\hat{\mathbf{r}} = \hat{x}\sin\psi\cos\alpha + \hat{y}\cos\psi - \hat{z}\sin\psi\sin\alpha \tag{21 a}$$

$$\hat{\mathbf{\Psi}} = \hat{x}\cos\psi\cos\alpha - \hat{y}\sin\psi - \hat{z}\cos\psi\sin\alpha \tag{21 b}$$

$$\hat{\boldsymbol{\alpha}} = -\hat{x}\sin\alpha - \hat{z}\cos\alpha \tag{21 c}$$

When projecting a torque acting on the layer normal along these bases vectors, i.e. by writing $\mathbf{\Gamma} = \Gamma_r\hat{\mathbf{r}} + \Gamma_\psi\hat{\mathbf{\Psi}} + \Gamma_\alpha\hat{\boldsymbol{\alpha}}$, one can give the following interpretation of the physical meaning of the spherical polar

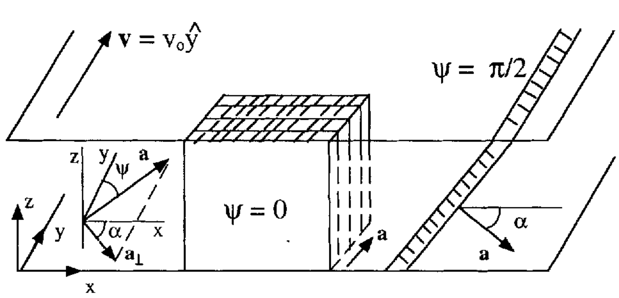

Figure 1. Definition of coordinates. The liquid crystal is confined between two glass plates, both parallel to the xy-plane. The upper one is moving in the y-direction, thus creating a velocity field $\mathbf{v} = v(z)\hat{y}$ in the liquid crystal. The orientation of the layer normal $\mathbf{a}$ is described by the polar angles ψ and α, where ψ is the angle between $\mathbf{a}$ and the y-axis, while α is the angle which the projection of the layer normal onto the xz-plane makes with the x-axis, counting α positive for rotations around the positive y-axis.

components of $\mathbf{\Gamma}$ [6]. The component Γ_r acts to rotate $\mathbf{a}$ around itself and will not influence the behaviour of the system. We will indeed show later that for all torques being calculated, the component Γ_r will identically equal zero. A torque component Γ_ψ tends to rotate the layer normal around the $\hat{\mathbf{\Psi}}$-axis, a rotation which decreases α keeping ψ constant. Correspondingly, a torque Γ_α rotates the layer normal around the $\hat{\boldsymbol{\alpha}}$-axis, a rotation which increases ψ while keeping α constant.

Finally, in order to achieve a feeling for how different layer orientations correspond to a specific choice of coordinates (ψ, α), study the right hand part of figure 1. When ψ is zero, the layers are standing up in the bookshelf geometry, the layer normal being parallel to the motion of the moving plate. Increasing ψ, the layer normal will gradually make a larger angle to this direction. For ψ equal to $\pi/2$, the layer normal will be perpendicular to the shearing direction, α being defined by the figure. This is the case when the flow does not necessitate any transport of matter from one layer to another.

3.2. *The rotational torque*

Neglecting the inertia of the system, the balance law for angular momentum is given by equation (9). As was discussed at the end of § 2, this equation can be interpreted as a balance of torque equation, where the torque furthermore can be divided into one part which is due to the rotational motion of the layers, while the other part is due to velocity gradients. Retaining only the terms which remain in the absence of velocity gradients, the rotational part of the antisymmetric stress tensor (16) is written

$$\tilde{t}^{\mathrm{ar}}_{ij} = \lambda_4(\dot{a}_j a_i - \dot{a}_i a_j). \tag{22}$$

Substituting the expression of $\mathbf{a}$ given by equation (20) into equation (22), the rotational torque is calculated from equation (17)

$$\Gamma^{\mathrm{r}}_x = 2\lambda_4(\dot{\psi}\sin\alpha + \dot{\alpha}\sin\psi\cos\psi\cos\alpha), \tag{23 a}$$

$$\Gamma^{\mathrm{r}}_y = -2\lambda_4\dot{\alpha}\sin^2\psi, \tag{23 b}$$

$$\Gamma^{\mathrm{r}}_z = 2\lambda_4(\dot{\psi}\cos\alpha - \dot{\alpha}\sin\psi\cos\psi\sin\alpha). \tag{23 c}$$

The spherical polar components of the rotational torque are now readily calculated from equations (21) and (23)

$$\Gamma^{\mathrm{r}}_{\mathrm{r}} = \mathbf{\Gamma}\cdot\hat{\mathbf{r}} = 0, \tag{24 a}$$

$$\Gamma^{\mathrm{r}}_\psi = \mathbf{\Gamma}\cdot\hat{\mathbf{\Psi}} = 2\lambda_4\dot{\alpha}\sin\psi, \tag{24 b}$$

$$\Gamma^{\mathrm{r}}_\alpha = \mathbf{\Gamma}\cdot\hat{\boldsymbol{\alpha}} = -2\lambda_4\dot{\psi}. \tag{24 c}$$

One notices that $\Gamma^{\mathrm{r}}_{\mathrm{r}}$ is zero, a result which is expected due to the symmetry of the system. As was discussed before, a rotation for which α decreases corresponds to a rotation around the positive ψ-axis. The rotational torque is a dissipative one, and must act to oppose any rotation, thus becoming negative in this case. From equation (24 *b*) it can be seen that for $\Gamma^{\mathrm{r}}_{\psi}$ to be negative when also $\dot{\alpha}$ is negative, one must demand λ_4 to be positive. In the same manner, one observes that a rotation for which ψ increases corresponds to a rotation around the positive α-axis, thus demanding the corresponding rotational torque to be negative. This again leads to the conclusion that λ_4 must be positive by inspection of equation (24 *c*). Thus the condition λ_4 be positive is a necessary one for the system to be stable, otherwise a fluctuation of the layer normal **a** would increase exponentially with a corresponding negative entropy production as a consequence. From the above discussion we also realise that λ_4 can be regarded as the rotational viscosity of the smectic layers.

3.3. *The shearing torque*

We now calculate the shearing torque, which is the torque acting on the layer normal if velocity gradients are present in the system. The set up of the shear flow is shown in figure 1, the velocity field and the layer normal being given by equations (19) and (20), respectively. Setting $\dot{\psi}$ and $\dot{\alpha}$ equal to zero, we obtain from equations (16), (17), (19) and (20),

$$\Gamma^{\mathrm{s}}_x = [-(\lambda_1+\lambda_4)\cos^2\psi + (\lambda_1-\lambda_4)\sin^2\psi\sin^2\alpha]v', \tag{25 a}$$

$$\Gamma^{\mathrm{s}}_y = (\lambda_1+\lambda_4)\sin\psi\cos\psi\cos\alpha\, v', \tag{25 b}$$

$$\Gamma^{\mathrm{s}}_z = (\lambda_1-\lambda_4)\sin^2\psi\sin\alpha\cos\alpha\, v'. \tag{25 c}$$

From equations (21) and (25) one can calculate the spherical polar components of the shearing torque as

$$\Gamma^{\mathrm{s}}_r = \mathbf{\Gamma}\cdot\hat{\mathbf{r}} = 0, \tag{26 a}$$

$$\Gamma^{\mathrm{s}}_\psi = \mathbf{\Gamma}\cdot\hat{\mathbf{\Psi}} = -(\lambda_1+\lambda_4)\cos\psi\cos\alpha\, v', \tag{26 b}$$

$$\Gamma^{\mathrm{s}}_\alpha = \mathbf{\Gamma}\cdot\hat{\boldsymbol{\alpha}} = (\lambda_4+\lambda_1\cos 2\psi)\sin\alpha\, v'. \tag{26 c}$$

One notices that the r-component of this torque is zero as expected. Furthermore, the physical interpretation of the torque components Γ^{s}_ψ and $\Gamma^{\mathrm{s}}_\alpha$ is that a positive torque component Γ^{s}_ψ will rotate the smectic layer normal in such a way that α decreases, while a positive torque component $\Gamma^{\mathrm{s}}_\alpha$ will act to increase ψ.

3.4. *The governing equations*

The governing equations of the system are the two equations for ψ and α determining the time evolution of the layer normal when the liquid is being subject to shear. These equations can be written down by summing up the total torque acting on the layer normal, and demanding that this be zero. From equations (24) and (26) we find that

$$2\lambda_4\dot{\alpha}\sin\psi - (\lambda_1+\lambda_4)\cos\psi\cos\alpha\, v' = 0, \tag{27 a}$$

$$-2\lambda_4\dot{\psi} + (\lambda_4+\lambda_1\cos 2\psi)\sin\alpha\, v' = 0. \tag{27 b}$$

Of the two viscous constants entering these equations we have proven λ_4 to be positive, being the rotational viscosity of the smectic layers. The other viscous constant, λ_1, must at this stage be allowed to adopt any value, and we show in the next two sections how the results derived there depend on the ratio λ_1/λ_4. These results are used in § 4 to make a reasonable guess about which values λ_1/λ_4 can be expected to adopt on physical grounds.

4. The flow alignment angles

In this section we derive the possible flow alignment angles of the system, i.e. we seek the orientations of the layer normal for which the shearing torque, equation (26), vanishes. To do so involves solving the equations

$$(\lambda_1+\lambda_4)\cos\psi\cos\alpha = 0, \tag{28 a}$$

$$(\lambda_4+\lambda_1\cos 2\psi)\sin\alpha = 0. \tag{28 b}$$

We also discuss how the smectic layers are oriented with respect to the shearing plane in the different cases. For some of the orientations corresponding to the solutions of equations (28), a small fluctuation of **a** creates a shearing torque which tends to rotate **a** away from the starting position. Although the torque is zero for such a solution, such an orientation is unstable and does not represent flow alignment of the system. However, we postpone the analysis of the stability of the solutions derived until the next section.

We now solve equations (28) and find readily that in terms of ψ and α there are three different solutions, which we denote **S**, **F** and **B** for reasons which become obvious later. We also remember that while λ_4 must always be positive, λ_1 can adopt any value.

(1) The **S** solution: $\psi=\pi/2$, $\alpha=0$. This solution corresponds to smectic layers in the bookshelf geometry with the layer normal perpendicular to the plane of shear. The solution exists for any value of λ_1, but we show in the next section that depending on the value of λ_1/λ_4, the solution exhibits three different types of stability. These three solutions are denoted $\mathbf{S}^-$, $\mathbf{S}^0$ and $\mathbf{S}^+$, respectively. Physically, these three solutions all have the same appearance, and are depicted in the upper part of figure 2.

(2) The $\mathbf{F}^-$ and $\mathbf{F}^+$ solutions: $\cos 2\psi = -\lambda_4/\lambda_1$, $\alpha=\pi/2$. These solutions exist only if $|\lambda_1|>\lambda_4$ and are depicted to the left in figure 2. The $\mathbf{F}^-$ solution corresponds to the choice of negative λ_1. Here the layer normal is confined within the shearing plane and the layers are tilted forward with a value of ψ which is less

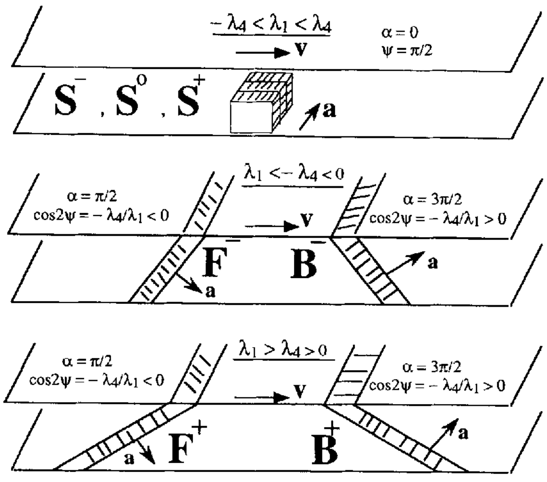

Figure 2. Equilibrium orientations of the smectic layers as they appear for different values of the ratio λ_1/λ_4. Not all of the depicted solutions to the stationary torque equations (28) represent stable equilibria.

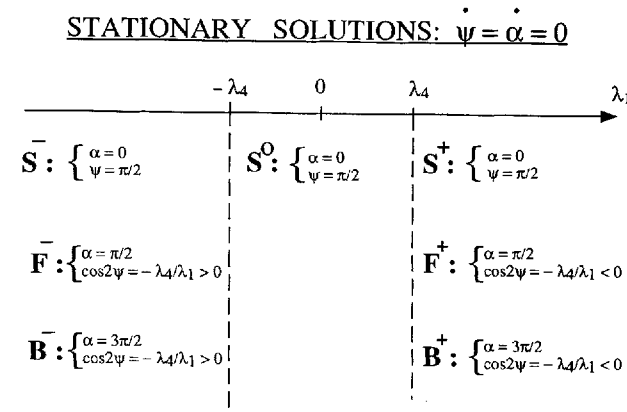

Figure 3. Summary and introduction of notations of the solutions to the stationary torque equations (28) as they are parametrized by the ratio λ_1/λ_4.

than $\pi/4$. the $\mathbf{F}^+$ solution corresponds to λ_1 being positive. The layer normal is also here confined within the shearing plane and the layer is tilted forward with a value of ψ in the range $\pi/4 < \psi < \pi/2$.

(3) The $\mathbf{B}^-$ and $\mathbf{B}^+$ solutions: $\cos 2\psi = -\lambda_4/\lambda_1$, $\alpha = 3\pi/2$. These solutions exist only if $|\lambda_1| > \lambda_4$ and are depicted to the right in figure 2. The $\mathbf{B}^-$ solution corresponds to the choice of negative λ_1. Here the layer normal is confined within the shearing plane and the layers are tilted backwards with a value of ψ which is less than $\pi/4$. The $\mathbf{B}^+$ solution corresponds to λ_1 being positive. The layer normal is also here confined within the shearing plane and the layer is tilted backwards with a value of ψ in the range $\pi/4 < \psi < \pi/2$.

To summarize, in terms of the value of λ_1/λ_4 one can distinguish three different regimes for the solutions of equations (28). Within each regime, different solutions are feasible as illustrated in figure 3. If $\lambda_1 < -\lambda_4$, the three solutions $\mathbf{S}^-$, $\mathbf{B}^-$ and $\mathbf{F}^-$ are all possible. When $-\lambda_4 < \lambda_1 < \lambda_4$, only the solution $\mathbf{S}^0$ is possible, while for $\lambda_1 > \lambda_4$ the three solutions $\mathbf{S}^+$, $\mathbf{B}^+$ and $\mathbf{F}^+$ can be found. In the next section we analyse the stability of these solutions in order to determine the possible orientations of the smectic layers in flow alignment.

5. Stability analysis

Figures 2 and 3 depict all possible orientations of the smectic layers, for which the shearing torque vanishes. We now analyse the stability of these in order to obtain the flow alignment angles of the layer normal.

5.1. *Linear stability analysis; the method*

Below we perform a linear stability analysis of equations (27) in the following way [7]. Given an equilibrium point (ψ_0, α_0) for which equations (27) are satisfied, we introduce two perturbation angles according to

$$\psi = \psi_0 + \gamma, \quad \alpha = \alpha_0 + \delta. \qquad (29\,a, b)$$

Expanding equations (28) for small values of γ and δ results in a set of linear differential equations with the structure

$$\dot{\gamma} = f_1(\gamma, \delta), \quad \dot{\delta} = f_2(\gamma, \delta). \qquad (30\,a, b)$$

These equations can be expressed in vector form as

$$\begin{pmatrix} \dot{\gamma} \\ \dot{\delta} \end{pmatrix} = \mathbf{A} \begin{pmatrix} \gamma \\ \delta \end{pmatrix}, \qquad (31)$$

the solution of which can be written

$$\begin{pmatrix} \gamma(t) \\ \delta(t) \end{pmatrix} = \exp(\mathbf{A}t) \begin{pmatrix} \gamma_0 \\ \delta_0 \end{pmatrix}, \qquad (32)$$

where γ_0 and δ_0 are the values of the perturbation for $t = 0$. It is the eigenvalues of the matrix $\mathbf{A}$, denoted by us ε_1 and ε_2, which determine the stability of the system [7]. If ε_1 and ε_2 are real and of the same signs the equilibrium point is a node, which is stable if $\varepsilon_i < 0$ and unstable if $\varepsilon_i > 0$. If ε_1 and ε_2 are real and of opposite signs, the equilibrium is a saddle point which is unstable. If the eigenvalues are complex with a negative real part, the equilibrium is a stable focus, while the equilibrium is an unstable focus if the real part is positive. When ε_1 and ε_2 are purely imaginary, the equilibrium point is a centre, which is stable. In the case when the equilibrium point is a stable node, the expression (32) represents an exponential decay towards the equilibrium point, characterized by two relaxation times, τ_1 and τ_2, which are given by [6]

$$\tau_1 = \frac{1}{|\varepsilon_1|}, \quad \tau_2 = \frac{1}{|\varepsilon_2|}. \qquad (33\,a, b)$$

5.2. *Investigation of the stability of the equilibrium points*

(1) The **S** solution: $\psi_0 = \pi/2$, $\alpha_0 = 0$. Substituting equations (29) into equations (27) leads to the following linearized set of equations for the time evolution of γ and δ,

$$\dot{\gamma} = \frac{v'}{2\lambda_4}(\lambda_4 - \lambda_1)\delta, \quad \dot{\delta} = -\frac{v'}{2\lambda_4}(\lambda_4 + \lambda_1)\gamma. \tag{34 a, b}$$

The eigenvalues of the matrix **A** are in this case given by

$$\varepsilon_i = \pm \frac{v'}{2\lambda_4}(\lambda_1^2 - \lambda_4^2)^{1/2}, \tag{35}$$

and the equilibrium is a saddle point (unstable) if $|\lambda_1| > \lambda_4$, while it is a centre (stable) if $|\lambda_1| < \lambda_4$. Thus the solutions $\mathbf{S}^-$ ($\lambda_1 < -\lambda_4$) and $\mathbf{S}^+$ ($\lambda_1 > \lambda_4$) are unstable while $\mathbf{S}^0$ ($-\lambda_4 < \lambda_1 < \lambda_4$) is stable and represents a possible flow alignment orientation.

(2) The $\mathbf{F}^-$ and $\mathbf{F}^+$ solutions: $\cos 2\psi_0 = -\lambda_4/\lambda_1$, $\alpha_0 = \pi/2$. Here one arrives at the following linearized version of equations (27),

$$\dot{\gamma} = -\frac{\lambda_1}{\lambda_4}\sin 2\psi_0\, v'\gamma, \quad \dot{\delta} = -\frac{(\lambda_4 + \lambda_1)}{2\lambda_4}\frac{\cos\psi_0}{\sin\psi_0}v'\delta, \tag{36 a, b}$$

and the corresponding eigenvalues of the matrix **A** are given by

$$\varepsilon_1 = -\frac{\lambda_1}{\lambda_4}\sin 2\psi_0\, v', \quad \varepsilon_2 = -\frac{(\lambda_4 + \lambda_1)}{2\lambda_4}\frac{\cos\psi_0}{\sin\psi_0}v'. \tag{37 a, b}$$

As ψ_0 is less than $\pi/2$, the three quantities $\sin\psi_0$, $\cos\psi_0$ and $\sin 2\psi_0$ are all positive and thus the signs of both the eigenvalues are opposite to that of λ_1, implying that the solution $\mathbf{F}^+$ ($\lambda_1 > \lambda_4$) is a stable node, while $\mathbf{F}^-$ ($\lambda_1 < -\lambda_4$) is an unstable node.

(3) The $\mathbf{B}^-$ and $\mathbf{B}^+$ solutions: $\cos 2\psi = -\lambda_4/\lambda_1$, $\alpha_0 = 3\pi/2$. Linearization of equations (27) yields

$$\dot{\gamma} = \frac{\lambda_1}{\lambda_4}\sin 2\psi_0\, v'\gamma, \quad \dot{\delta} = \frac{(\lambda_4 + \lambda_1)}{2\lambda_4}\frac{\cos\psi_0}{\sin\psi_0}v'\delta, \tag{38 a, b}$$

the eigenvalues of the matrix **A** being given by

$$\varepsilon_1 = \frac{\lambda_1}{\lambda_4}\sin 2\psi_0\, v', \quad \varepsilon_2 = \frac{(\lambda_4 + \lambda_1)}{2\lambda_4}\frac{\cos\psi_0}{\sin\psi_0}v'. \tag{39 a, b}$$

Now the signs of both the eigenvalues are the same as that of λ_1, implying that the solution $\mathbf{B}^-$ ($\lambda_1 < -\lambda_4$) is a stable node, while $\mathbf{B}^+$ ($\lambda_1 > \lambda_4$) is an unstable node.

5.3. *Summary*

Figure 4 summarizes the results, depicting all possible solutions of equations (28) parametrized by the value of λ_1/λ_4. Moving from the left to right in the figure λ_1 increases, the two dashed vertical lines corresponding to λ_1 equal to $\pm\lambda_4$. For each value of λ_1 there is one or three solutions to equations (28), one of these being stable while the other two (if they exist) being unstable.

In all cases of the three **S** solutions will exist, corresponding to smectic layers in the bookshelf geometry with the layer normal perpendicular to the plane of shear. Only if $|\lambda_1| < \lambda_4$ the solution $\mathbf{S}^0$, which in this case is a centre, is stable. In the other two cases, $|\lambda_1| > \lambda_4$, the two solutions $\mathbf{S}^-$ and $\mathbf{S}^+$ are unstable, in each case being a saddle point.

When $\lambda_1 \geqslant \lambda_4$ there are also the $\mathbf{B}^+$ and $\mathbf{F}^+$ solutions. In the limiting case $\lambda_1 \to \lambda_4$, both these solutions represent layers which are parallel to the bounding plates. When λ_1 increases the layers start to tilt, either forwards or backwards, with an increasing angle which in the limiting case $\lambda_1 \to \infty$ equals $\pi/4$. Of these two solutions $\mathbf{B}^+$ represents an unstable node while $\mathbf{F}^+$ is a stable node.

When $\lambda_1 \leqslant -\lambda_4$ the two additional solutions are the $\mathbf{B}^-$ and $\mathbf{F}^-$ solutions. In the limiting case $\lambda_1 \to -\lambda_4$, both these solutions represent standing layers in the bookshelf geometry, the layer normal of which being parallel to the velocity of the moving plate. When λ_1

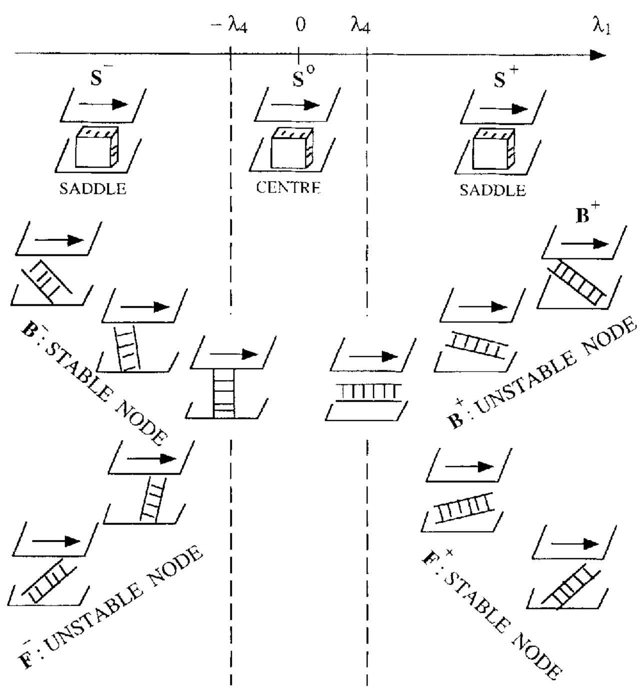

Figure 4. Equilibrium orientations of the smectic layers in shear flow. In the figure is indicated which type of stability the solutions exhibit and also how the orientations of the layers depend on the ratio λ_1/λ_4.

decreases the layers start to tilt, either forwards or backwards, with an increasing angle which in the limiting case $\lambda_1 \to -\infty$ equals $\pi/4$. Of these two solutions $\mathbf{B}^-$ represents a stable node while $\mathbf{F}^-$ is an unstable node.

6. Comparison with disc-like nematics: proposition for the value of λ_1

Figure 4 presents all possibilities for flow alignment, including the corresponding stability conditions. As is seen, the value of λ_1 is crucial for the behaviour of the system. Before any experimental values of this viscous coefficient have been obtained, it is hard to make any reliable predictions as to how the system behaves in reality. However, by observing that the smectic layers can be regarded as infinite discs, one can compare the results of figure 4 with the more established behaviour of disc-like nematic liquid crystals being subject to shear [8, 9]. The latter system can exhibit one of two types of behaviour, depending on the values of two viscous constants, denoted α_2 and α_3. The director, which in this case is the normal to the discs, corresponding to the layer normal in the present problem, will for some parameter values orient itself perpendicular to the plane of shear. This behaviour corresponds to the $\mathbf{S}^0$ solution in figure 4. For other parameter values, the disc-like nematics exhibit flow alignment with the director in the plane of shear, the discs making a small angle to the bounding plates. This situation resembles the $\mathbf{F}^+$ solution if one chooses λ_1 to be positive and slightly larger than λ_4.

From consideration of the above discussion of the behaviour of disc-like nematics in shear, how would one expect a S_A liquid crystal to behave in a similar situation? One can of course argue that the smectic layers, being infinite discs, can only exhibit the $\mathbf{S}^0$ type of solution if one demands the smectic layers to stay intact, thus favouring the choice $|\lambda_1| < \lambda_4$. However, if the smectic layers break up into smaller units, the system being transformed into some kind of discotic smectic, the solutions exhibiting a layer normal within the plane of shear should also be able to exist (it is beyond the scope of this work to discuss the nature of the defects by which this inevitably must be accompanied). Comparing with the behaviour of a disc-like nematic under similar circumstances, one then expects the $\mathbf{F}^+$ solution, with $\lambda_1 \gtrapprox \lambda_4$, to be the one exhibited by the system. How the system behaves in reality has to be decided by experimental investigations, but it seems to us that the symmetry of the system would favour either the $\mathbf{S}^0$ $(-\lambda_4 < \lambda_1 < \lambda_4)$ or $\mathbf{F}^+$ (with $\lambda_1 \gtrapprox \lambda_4$) type of behaviour. Possibly, as for nematics, both types of behaviour, depending on which substance is being studied, could be expected to be observed.

7. Balance of linear momentum: the effective viscosities

In this section we write down the equations for balance of linear momentum in shear flow, employing the result to derive the effective viscosities in some special cases. By this procedure we can derive a few additional inequalities for the viscous constants of the system. Consider the three cases depicted in figure 5. Either the system is in the bookshelf geometry, the layer normal being perpendicular (*a*) or parallel (*b*) to the velocity of the moving plate, or the smectic layers are assumed to be parallel to the bounding plates (*c*). Although these geometrical arrangements of the smectic layers may not all correspond to the equilibrium situations depicted in figure 4, one can always assume some external torque (i.e. boundary conditions, electric or magnetic fields) to stabilize the assumed configuration in the presence of flow.

Moving the upper plate in the *y*-direction, the equation for balance of linear momentum (8) reads in the steady state,

$$\tilde{t}_{yz,z} = 0, \tag{40}$$

which can be integrated to read

$$\tilde{t}_{yz} = \tau, \tag{41}$$

the integration constant τ being the force per unit area applied to the moving plate. The stress tensor, defined by equations (15) and (16), together with equations (10)–(13) and the velocity field (19) now gives

$$v' = \frac{\tau}{\eta_i}, \tag{42}$$

where η_i is the effective viscosity, which for the three different cases studied is given by

$$\mathbf{a} = \hat{\mathbf{x}}: \quad \eta_a = \tfrac{1}{2}\mu_0 > 0, \tag{43 a}$$

$$\mathbf{a} = \hat{\mathbf{y}}: \quad \eta_b = \tfrac{1}{2}(\mu_0 + \mu_2 + 2\lambda_1 + \lambda_4) > 0, \tag{43 b}$$

$$\mathbf{a} = \hat{\mathbf{z}}: \quad \eta_c = \tfrac{1}{2}(\mu_0 + \mu_2 - 2\lambda_1 + \lambda_4) > 0, \tag{43 c}$$

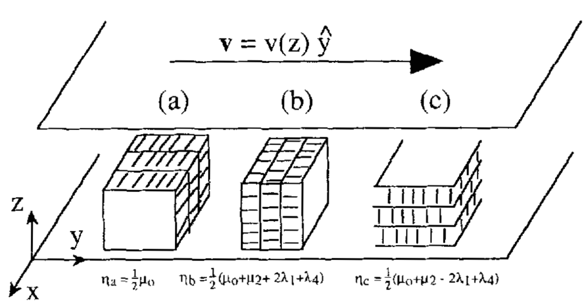

Figure 5. Definition of the effective viscosities η_a (bookshelf geometry; layer normal perpendicular to shear plane), η_b (bookshelf geometry: layer normal parallel to the fluid velocity) and η_c (layers parallel to the bounding plates: layer normal parallel to the shear).

the inequalities in equations (43) stemming from the fact that the velocity gradient v' and the driving force τ must be of the same sign. We take the inequalities (43 *b*) and (43 *c*) a little further by rewriting them as

$$2\lambda_1 > -(\mu_0 + \mu_2 + \lambda_4), \quad 2\lambda_1 < \mu_0 + \mu_2 + \lambda_4. \qquad (44\,a, b)$$

If these inequalities both hold at the same time, one must demand

$$\mu_0 + \mu_2 + \lambda_4 > 0. \qquad (45)$$

Equations (44) can be summarized as

$$|2\lambda_1| < \mu_0 + \mu_2 + \lambda_4. \qquad (46)$$

Thus some of the inequalities, which on thermodynamic grounds must be fulfilled by the viscous constants, can be summarized as

$$\lambda_4 > 0, \quad \mu_0 > 0, \quad \mu_0 + \mu_2 + \lambda_4 > 0, \qquad (47\,a, b, c)$$

$$|\lambda_1| < \tfrac{1}{2}(\mu_0 + \mu_2 + \lambda_4). \qquad (47\,d)$$

8. Discussion

In this paper we have discussed the macroscopic flow properties of the S_A phase with the stress tensor given by equations (15) and (16) as a starting point. We have assumed the orientation of the smectic layers to be arbitrary, an assumption which in some cases leads to a flow for which matter has to be transported between the smectic layers. This assumption might place some restriction on the validity of the results thus derived. However, we believe that, as a starting point for investigating the dynamics of the S_A phase, the present approach is a reasonable one. Also, regarding the possibility for the smectic layers to break up into smaller units, as was discussed in § 5.3, the apparent discrepancy between the smectic layering and the flow field becomes weaker.

With the above limitations in mind, the possible orientations of free smectic layers in shear flow are summarized in figure 4, from which one notices that the results depend critically on the viscosity coefficient λ_1. From a comparison with the behaviour of disc-like nematics in shear flow, one observes similarities which can be used to make predictions of the value of λ_1. Our assumption is $\lambda_1 > -\lambda_4$, possibly most likely with $\lambda_1 \gtrapprox \lambda_4$ being valid. From equation (47 *d*), the value of λ_1 is seen also to have an upper limit due to the inequality $|\lambda_1| < \frac{1}{2}(\mu_0 + \mu_2 + \lambda_4)$. As the value of μ_2 is still completely undetermined, one cannot draw too strong conclusions from this inequality; however the assumption $\lambda_1 \gtrapprox \lambda_4$ remains a realistic choice as well as $|\lambda_1| < \lambda_4$. In the end however, experiments will decide which values the viscous constants adopt in reality.

References

[1] LESLIE, F. M., STEWART, I. W., and NAKAGAWA, M., 1991, *Mol. Cryst. liq. Cryst.*, **198,** 443.
[2] CARLSSON, T., LESLIE, F. M., and CLARK, N. A., 1995, *Phys. Rev. E*, **51,** 4509.
[3] CARLSSON, T., CLARK, N. A., and ZOU, Z., 1993, *Liq. Cryst.*, **15,** 461; errata: *Liq. Cryst.*, **17,** 147.
[4] ZOU, Z., CLARK, N. A., and CARLSSON, T., 1994, *Phys. Rev. E*, **49,** 3021.
[5] DE GENNES, P. G., 1975, *The Physics of Liquid Crystals* (Oxford: Clarendon Press).
[6] CARLSSON, T., 1986, *Phys. Rev. A*, **34,** 3393.
[7] See, e.g. MEIROVITCH, L., 1975, *Elements of Vibrational Analysis* (New York: McGraw-Hill), chapter 9.3.
[8] CARLSSON, T., 1982, *Mol. Cryst. liq. Cryst.*, **89,** 57.
[9] CARLSSON, T., 1983, *J. de Physique*, **44,** 909.